3

Synthesis and morphology control of Eu^{3+} doped M_2O_2S [M=Y, Gd] nanostructures

Rathinam Chandramohan, Jagannathan Thirumalai
and Thirukonda Anandamoorthy Vijayan
Department of Physics,Sree Sevugan Annamalai College,Devakottai - 630 303
India

1. Introduction

Global claim for phosphor materials as efficient sources of energy that can supply sustained competence is growing day by day. The phosphors are facing increased global challenges including high production of rare earth materials, environmental and recycling issues, and necessity to supply devices very quickly that may be outdated rapidly due to new technological developments arising in the industry and market. A number of applications have emerged in recent years that will change the future of the industry and new technologies like nanoscale innovations and specialty phosphors are garnering increased attention. The primary drivers for growth are the expansion of key end-use applications including solid-state lighting and fluorescent lighting. Current research in nanotechnology is focused on new materials, novel phenomena, new characterization technique and fabrication of nano devices.

$Y_2O_2S:Eu^{3+}$ and $Gd_2O_2S:Eu^{3+}$ are excellent materials of current interest (Lei et al., 2010; Liu & Kuang, 2010; Li, et al., 2010; Nakkiran et al., 2007; Thirumalai et al., 2007) owing to their interesting optical and opto-electronic properties. The crystal structure of M_2O_2S (M = Y, Gd and including all lanthanides) are discussed in detail (Delgado da Vila et al., 1997; Sabot & Maestro, 1995; Mikami & Oshiyama, 1998). The crystal symmetry of the above two systems is trigonal, with the space group P3m1 (D^3_{3d}), as determined by X-ray diffraction. These systems are grouped under wide band gap (4.6 – 4.8 eV) semiconductors. $Y_2O_2S:Eu^{3+}$ and $Gd_2O_2S:Eu^{3+}$ as a red phosphor, with its sharp emission line for good calorimetric definition and high luminescence efficiency, is extensively used in the phosphor screen of display devices, fluorescent lamps used for lighting purposes, television sets used for entertainment and information gathering, X-ray imaging instruments used in hospitals and laser instruments used for experimental purposes and, many other electrical and opto-electronic equipments. They employ luminescent materials for (Nakkiran et al., 2007) electronic portal imaging devices (EPID), radioisotope distribution and so on (Yeboah & Pistorius, 2000; Chou et al., 2005). Due to the large size and weight of CRTs, developments of flat-panel displays (FPDs) are of great interest. Among several FPD technologies, liquid-crystal displays (LCDs) dominate the FPD market and plasma display panels (PDPs) are now commercially available in the large area TV market (Yu et al., 2005). New and enhanced

properties are expected due to size confinement in nanoscale dimensions that can revolutionize the display devices market in future. Commercially available bulk oxysulfides are quite expensive and are not easily available. So, for the time being, $Y_2O_2S:Eu^{3+}$ and $Gd_2O_2S:Eu^{3+}$ nanostructures are relatively a good choice while compared with the bulk systems. However, for an extensive use in the commercial applications, $Y_2O_2S:Eu^{3+}$ and $Gd_2O_2S:Eu^{3+}$ nanocrystals must be prepared at lower temperatures. Therefore, it is necessary to develop a low-temperature synthesis technology for the growth of oxysulfide nanophosphors. In this background, this chapter has been devoted to the nanophosphors development using these two systems. The realm of novel devices from this wonderful material is yet to be accomplished in full. To give a quantitative report on the state of art of $Y_2O_2S:Eu^{3+}$ and $Gd_2O_2S:Eu^{3+}$ is quite difficult and an attempt has been made to give an account of the synthesis of the nanophosphors in this chapter.

A detailed survey on Y_2O_2S: Eu^{3+} and Gd_2O_2S: Eu^{3+} nanophosphors discusses various synthesis techniques adopted by different research groups as follows. Powder phosphors of $(Y_{1-X}RE_X)_2O_2S$, $(Gd_{1-X}RE_X)_2O_2S$ and $(La_{1-X}RE_X)_2O_2S$ where RE=Eu^{3+}, Tb^{3+}, or Tm^{3+} that were prepared by combustion reactions from mixed metal nitrate reactants and dithiooxamide $(CSNH_2)_2$ with ignition temperatures of 300 – 350 ^oC (Bang et al., 2004). The $Y_2O_2S:Eu^{3+}$ red phosphor which was prepared by a new method of decomposing the metal complexes $Y(NO_3)_3 \bullet 3(DMSO)$ and $Eu(NO_3)_3 \bullet 4(DMSO)$ in H_2S atmosphere at 900 ^oC (Guo et al., 2008). Nanocrystalline $Y_2O_2S:Eu^{3+}$ was successfully prepared using a combustion synthesis method employing conventional sulfur flux (Fu et al., 2008). A method of preparing red emitting Eu^{3+}:Y_2O_2S phosphors in which Yttrium sulfite doped Eu is used as starting material and the Eu-activated oxysulfide is obtained from either directly by reducing the sulfite with carbon monoxide, or by first oxidizing sulfite and then reducing the obtained oxysulfate (Koskenlinn et al., 1976). Preparation of spherical Y_2O_2S and Y_2O_2S:Eu particles using a solid–gas reaction of monodispersed precursors with elemental sulfur vapor under an argon atmosphere has been investigated (Delgado da Vila et al., 1997). A one-step solvothermal process developed for the preparation of Eu^{3+} actived yttrium oxysulfide phosphor in ethylenediamine solvent at 280°C through a reaction of yttrium oxide, europium oxide, and sulfur powder (Kuang et al., 2005). Luminescent $Y_2O_2S:Eu^{3+}$ nanoceramics prepared through a gel–polymer thermolysis process employing a urea–formaldehyde resin (Dhanaraj et al., 2003). Nanocrystals of $Y_2O_2S:Eu^{3+}$ synthesized using a two step sol–gel polymer thermolysis method (Dhanaraj et al., 2004). Ensembles of $Y_2O_2S:Eu^{3+}$ widegap semiconductor nano-crystals exhibit ON–OFF fluorescence blinking phenomenon, which mimic II–VI semiconductor quantum-structures synthesized using sol-gel polymer thermolysis method (Thirumalai et al., 2007). Trivalent europium-doped yttrium oxysulfide nanocrystals synthesized using sol–gel thermolysis. A significant blue shift observed in the fundamental absorption edge for the nanocrystals having an average crystallite size (f) in the range 9–15nm indicated a strong quantum confinement with a Bohr exciton radius of 5–13 nm (Thirumalai et al., 2007; Thirumalai et al., 2008). The $Y_2O_2S:Eu^{3+}$ nanocrystallines that were prepared by a new ethanol assisted combustion synthesis method using sulfur contained organic fuel (thioacetamide) in an ethanol-aqueous solution (Xixian et. al., 2006). The luminescence dynamics of optical centers in nanocrystals depending critically on the phonon density of states (PDOS) is quite distinct from that of bulk materials. It is shown that energy transfer (ET) in nanocrystals is confined by discrete PDOS as well as direct size restriction. For applications, the nanoconfinement effects on ET

significantly reduce the efficiency of sensitized or upconversion luminescence (Chen et. al., 2003). The Y_2O_2S:Eu phosphor powders were prepared with a flux fusion method and electrophoretically deposited on an ITO-coated glass substrate to form a thin layer (Tseng et al., 1998). The nanostructured yttrium oxysulfide films prepared via vapor phase growth (V. V. Bakovets et al., 2008). Their first step was the deposition of 50-nm-thick nanostructured yttria films from yttrium dipivaloylmethanate vapor at 525 ^oC. Next, the films were sulfided in ammonium thiocyanate vapor at temperatures from 800 to 1100 ^oC. Hexagonal yttrium oxysulfide was obtained at 900 ^oC and higher temperatures. The investigations of pseudobinary systems Ln_2O_2S---La_2O_2S (*Ln* = Nd, Sm, Eu, Gd, Dy, Yb, Lu, and Y) with complete solid solubility only for the systems like Nd_2O_2S---La_2O_2S and Sm_2O_2S---La_2O_2S; a two-phase region is found for all other systems (M. Leskelä et al., 1976). The solid solubility in the isostructural oxysulfide series is discussed in terms of the differences in ionic radii of the two rare-earth components. The size- (submicrometer-sized) and morphology- (spherical) controlled composite Gd–Eu oxalate particles were prepared in an emulsion liquid membrane (water-in-oil-in-water emulsion) system (Hirai et al., 2002). The oxalate particles thus prepared were calcined in air to obtain Gd_2O_3:Eu^{3+} phosphor particles and in sulfur atmosphere to obtain Gd_2O_2S : Eu^{3+} phosphor particles.
Usually synthesis of any phosphor material would necessitate rigorous conditions such as heavy milling, intermediate and very high temperature heat treatment cycles, etc. Whereas the hydrothermal approach avoids all those difficult and time consuming steps by modifying the reaction parameters to suitable forms so as to react and produce target compound(s) at relatively lesser duration with the capacity to develop desired shapes and dimensions with high crystallanity. The Y_2O_2S:Eu^{3+} and Gd_2O_2S:Eu^{3+} nanostructures show optimum properties (perfect crystalline structure, high stability and good morphological) when they are grown on perfect hydrothermal conditions. In addition to the conventional vapor-phase method, which includes vapor transport and condensation (Kong et al., 2001), metal-organic chemical vapor deposition (Zhang et al, 2004), thermal evaporation (Pan et al, 2001) and solution-phase methods have been developed as alternative ways to synthesize semiconductor nanostructures with different shapes and dimensions. Hydrothermal method is a widely used technique that can control the shape and dimension of nanostructures among all solution-based approaches (Zhang et al, 2002). Unlike conventional vapor-phase methods, the hydrothermal method can produce various nanostructures at a relatively low temperature (below 200 °C) using simple equipments; however, the reaction time required for the growth of nanostructures is too long (usually from a few hours to several days) (Wang & Li, 2003; Wang et al, 2003; Zhang et al, 2002). The various low-dimensional nanostructures, such as nanowires, nanotubes, nanosheets and fullerene like nanoparticles that have been selectively synthesized from rare-earth compounds (hydroxides, fluorides) based on a facile hydrothermal method (Wang & Li, 2003; Wang et al, 2003). The subsequent dehydration, sulfidation and fluorination processes lead to the formation of rare-earth oxide, oxysulfide and oxyhalide nanostructures, which can be functionalized further by doping with other rare-earth ions. An effective method to synthesize Y_2O_2S:Eu^{3+}, Mg^{2+}, Ti^{4+} nanoparticles. Tube-like $Y(OH)_3$ were firstly synthesized by hydrothermal method to serve as the precursor. Nanocrystalline long-lasting phosphor Y_2O_2S:Eu^{3+}, Mg^{2+}, Ti^{4+} was obtained by calcinating the precursor with co-activators and S powder (Li, et. al., 2010). The afterglow properties of Eu^{3+} activated long lasting Gd_2O_2S phosphor by hydrothermal route. Rod-like $Gd(OH)_3$

were firstly synthesized by hydrothermal method to serve as the precursor. Long lasting $Gd_2O_2S:Eu^{3+},Ti^{4+},Mg^{2+}$ phosphor were obtained by calcinating the precursor with co-activators and S powder (Hang et al., 2008). Hydrothermally prepared $Gd(OH)_3$ nanorod precursor, codoped with Eu, Ti and Mg, was converted into the desired phosphor by calcinating the precursor in CS_2 atmosphere (Mao et al., 2008). Therefore, the development of a simple and fast synthetic route that can control the shape of nanostructures under ambient conditions is the need of the hour and hydrothermal technique has many advantages and technological possibilities. Earlier (Wang & Li, 2003; Wang et al, 2003; Hang et al., 2008; Mao et al., 2008) hydrothermal method was used to synthesize oxysulfide nanotubes and nanorods.

To the best of the author's knowledge, no systematic study has been reported on other nanostructures like nanocrystals, nanosheets, nanobelts, nanotubes, nanorods, nanowires and nanoflowers of this oxysulfide system (Thirumalai et al, 2008; Thirumalai et al, 2009 a, b). Hence maximum efforts were to be put forth in selecting techniques for the synthesis of various nansostructures with good crystallinity, so also any other oxysulfide nanostructures of high research potential activity. Therefore, the present study has been undertaken with a view to synthesizing uncontaminated, highly crystalline $Y_2O_2S:Eu^{3+}$ and $Gd_2O_2S:Eu^{3+}$ adopting two methods of hydrothermal routes owing to the relatively lower temperature with respect to the bulk counterpart (solid-state reaction method): **Template – free method** (two-step synthesis) involving the synthesis of as-prepared $Y(OH)_3$ and $Gd(OH)_3$, followed by subsequent Eu^{3+} doping and sulfurization leading to conversion of $Y_2O_2S:Eu^{3+}$ and $Gd_2O_2S:Eu^{3+}$ nanostructures, respectively, seemed to be a topotactic reaction. **Template – assisted method** (single-step synthesis) involving Anodic Aluminium Oxide (AAO) membranes used for synthesizing of $Y_2O_2S:Eu^{3+}$ and $Gd_2O_2S:Eu^{3+}$ nanostructures. Furthermore, being a low temperature and an easy-to-adopt methodology, this method yields phase pure $Y_2O_2S:Eu^{3+}$ and $Gd_2O_2S:Eu^{3+}$ nanostructures with better reproducibility, definite shape and dimensions. Hydrothermal method is basically a simple, easy and fast synthetic route where the most important synthesis parameters are the precursors, the solution concentration, solution pH value, solvent, temperature and time. Also, this processing route provides the basis for a nearly low cost, low temperature method for the preparation of homogeneous nano-sized ceramics compared to any other existing methods.

2. Formation, structure, and morphology of the $Y_2O_2S:Eu^{3+}$ and $Gd_2O_2S:Eu^{3+}$ nanostructures

2.1 Template – free Method

A systematic study has been undertaken on other nanostructures like nanocrystals, nanosheets, nanobelts, nanotubes, nanorods, nanowires and nanoflowers by varying reaction parameters such as solution concentration, pH, growth temperature and reaction time and solvent using template-free method. The effect of these parameters are studied using various characterization studies and the optimized reaction conditions are arrived for $Y_2O_2S:Eu^{3+}$ and $Gd_2O_2S:Eu^{3+}$ nanostructures. The detailed synthesis procedure is discussed already in detail (Thirumalai et al, 2008; Thirumalai et al, 2009 a, b).

Structural studies (XRD) reveal that the products $Y_2O_2S:Eu^{3+}$ and $Gd_2O_2S:Eu^{3+}$ are pure hexagonal phase and they are in good agreement with standard JCPDS [($Y_2O_2S:Eu^{3+}$;

JCPDS # 24-1424) and ($Gd_2O_2S:Eu^{3+}$; JCPDS # 26-1422)] data (Thirumalai et al, 2008; Thirumalai et al, 2009 a, b) and they are highly crystalline in nature. It is already stated that, the conversion from hydroxide to oxysulfide seems to be a topotactic reaction. Firstly, the hydroxide(s) [$Y(OH)_3$ and $Gd(OH)_3$] of nanocrystals / nanoplates, nanosheets, nanobelts, nanotubes, nanorods and nanowires are selectively synthesized were based on the preparation of colloidal hydroxide precipitates at room temperature, and the subsequent hydrothermal treatment at 100 – 180 ^oC for approximately 12 – 48 hours (Thirumalai et al, 2008; Thirumalai et al, 2009 a, b). The hydrothermal method was shown to be effective in the synthesis of zero- and one-dimensional nanostructures. By the simple tuning of factors such as pH, temperature and concentration, the experimental conditions could be chosen to favor the anisotropic growth of materials. In the present work, nanostructures of hydroxide(s) were successfully obtained through this precipitation–hydrothermal synthetic method by properly tuning the temperature, pH and time, the crystal structures have been found to be responsible for the growth of hydroxide nanostructures with nearly controllable aspect ratios. The conversion of hydroxide to oxysulfide seems to be a topotactic reaction (i.e., the morphology does not change while the phase of the material changes). However in any topotactic reactions, where significant atomic rearrangement due to chemical changes take place, though the morphology remains intact. Yet it is possible to change the resulting morphology. With this important criteria the as-synthesized $Y(OH)_3$ and $Gd(OH)_3$ were converted to $Y_2O_2S:Eu^{3+}$ and $Gd_2O_2S:Eu^{3+}$ nanostructures. To investigate the optimized growth of the $Y_2O_2S:Eu^{3+}$ and $Gd_2O_2S:Eu^{3+}$ nanostructures, SEM and TEM (Thirumalai et al, 2008; Thirumalai et al, 2009 a, b) micrographs of nanocrystals, nanosheets, nanobelts nanotubes, nanorods and nanowires, respectively, were obtained by varying the reaction parameters (pH ~ 6 – 13, 100 – 180 °C, 24 – 48 hrs) and its resulting morphological features and crystallanity are found to be good and were discussed in Table I (Thirumalai et al, 2009 a, b). The studies reveal that by altering the reaction conditions (like solution concentration, pH, temperature and time) the morphology, shape and crystallinity may be perfectly controlled. The SEM and TEM results are discussed and presented in Fig. 1-4. Fig. 1a, 2a and Fig. 3b, 4b show that growth is clearly seen indicating the nanocrystals formed due to combination of spherical and hexagonal-like structure at a pH of 6, 100°C, 48 hrs, respectively. Fig. 1b, 2b and Fig. 3c, 4c show stacked nanosheets of the oxysulfide(s) growth at pH ~ 8, 120°C, 12 hrs, respectively. This may be attributed to the two-dimensional growth tendency of the oxysulfide(s) nanosheets at lower pH. Nevertheless, Fig. 1c, 2c and Fig. 3d, 4d, show the nanobelts of $Y_2O_2S:Eu^{3+}$ and $Gd_2O_2S:Eu^{3+}$ grown at a pH of 8 – 9, 180°C, 24 hrs, respectively. These nanosheets and/or nanobelts curl from the edge, indicating a possible rolling process for the formation of the nanotubes/rods/wires. Fig. 1(d, e, f), 2(d, e, f) and Fig. 3(e, f, g), 4(e, f, g) show that the nanotubes, rods, wires were grown at a pH of 12 – 13, 140 – 180°C, 24 – 48 hrs and has no template to drive the directional growth of nanotubes, rods and wires. The images indicate that the samples are single crystalline in nature and uniformly distributed. Also, based on the above studies it is evident that these nanostructures are stable under thermal treatment, which may be rather useful for their subsequent applications as catalysts. Furthermore, the morphology of these nanostructures is likely to be a near-quantum structure. It is having high surface-to-volume ratio, that plays a major role in the density of singly ionized oxygen vacancies and the charge state of these defects, that may be due to the existence of surface depletion.

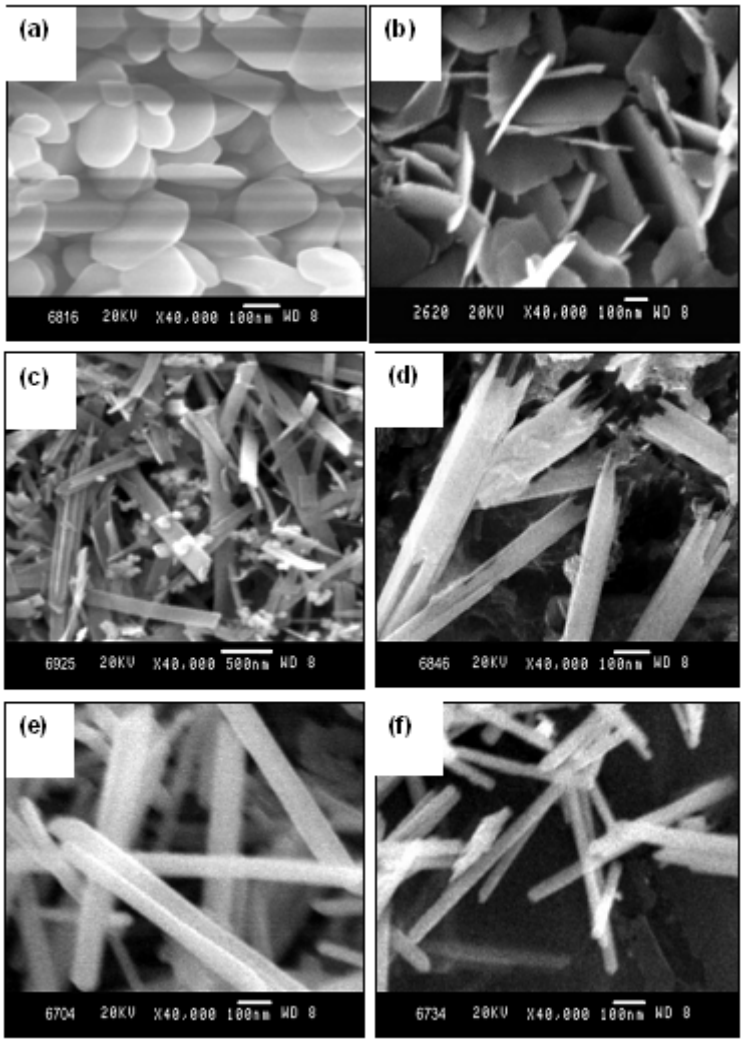

Fig. 1. SEM images show the optimal experimental conditions of $Y_2O_2S:Eu^{3+}$ nanostructures using template – free method.

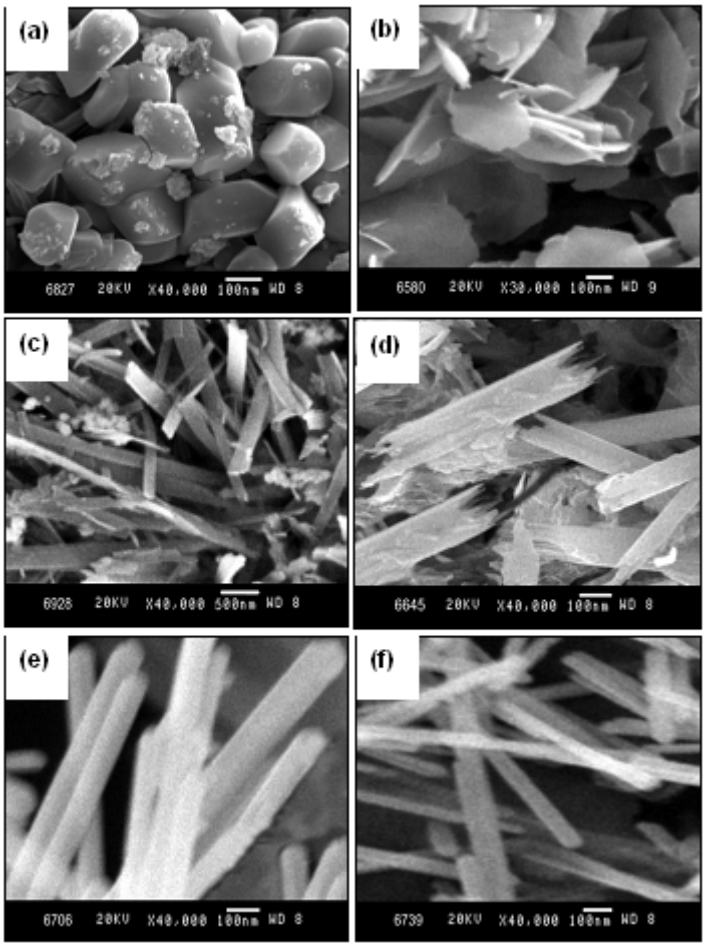

Fig. 2. SEM images show the optimal experimental conditions of $Gd_2O_2S:Eu^{3+}$ nanostructures using template – free method.

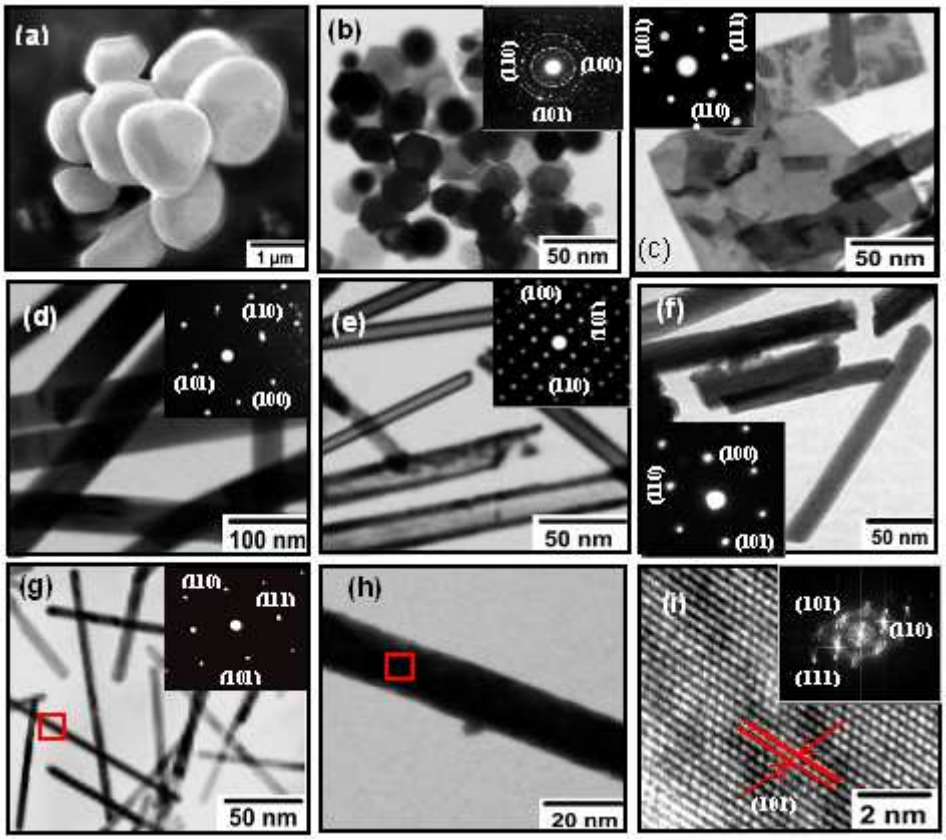

Fig. 3. (a) SEM image of hexagonal-shaped bulk $Y_2O_2S:Eu^{3+}$ (A). The TEM images of $Y_2O_2S:Eu^{3+}$ nanostructures (template – free method) from the sample A_7 to A_{12}: (b) Nanocrystals, (c) Nanosheets, (d) Nanobelts, (e) Nanotubes, (f) Nanorods, (g) Nanowires, (h) a close up of the boxed area in (g) shows a structure of single-nanowire, (i) HRTEM image of $Y_2O_2S:Eu^{3+}$ nanowire. *Courtesy: J. Colloid. Interface. Sci. 336., 2., (2009) 889-897.*

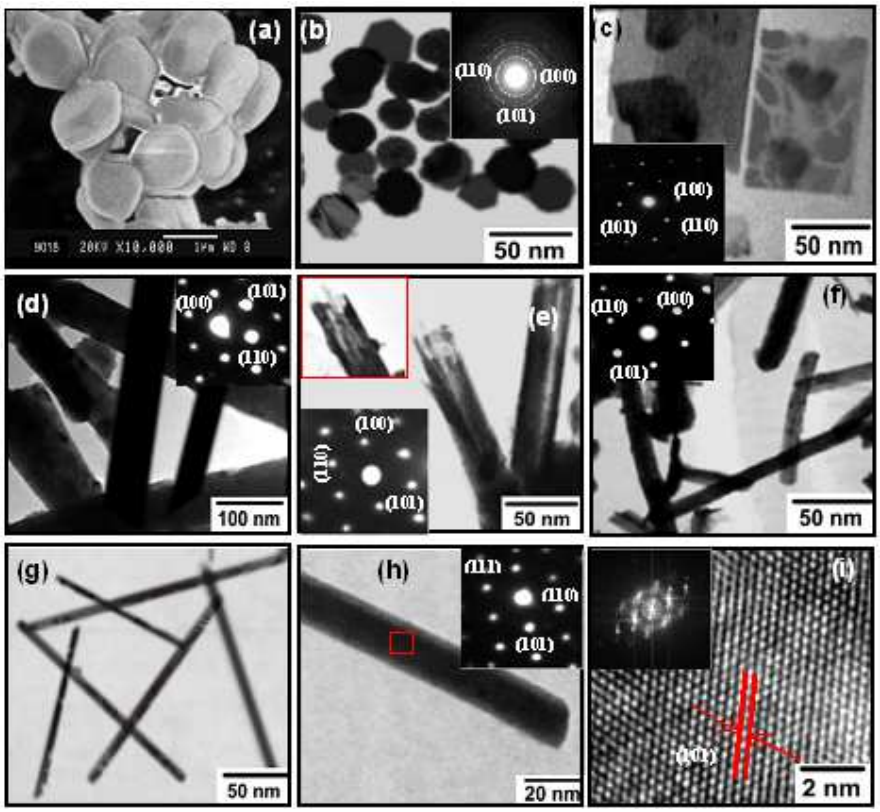

Fig. 4. (a) SEM image of hexagonal-shaped bulk $Gd_2O_2S:Eu^{3+}$ (B). The TEM images of $Gd_2O_2S:Eu^{3+}$ nanostructures (template – free method) from the sample B_7 to B_{12}: (b) Nanocrystals, (c) Nanosheets, (d) Nanobelts, (e) Nanotubes (inset: shows TEM image of the end portion of a single-nanotube), (f) Nanorods, (g) Nanowires, (h) a close up of the boxed area in (g) shows a structure of single-nanowire, (i) HRTEM image of $Gd_2O_2S:Eu^{3+}$ nanowire. The spacing between two adjacent lattice planes is 0.325 nm, which corresponds to the separation of the hexagonal phase lattice planes (110), and the inset shows Fast Fourier transform (FFT) pattern of the corresponding nanowire. *Courtesy: J. Mater. Sci. 44., 14., (2009) 3889-3899.*

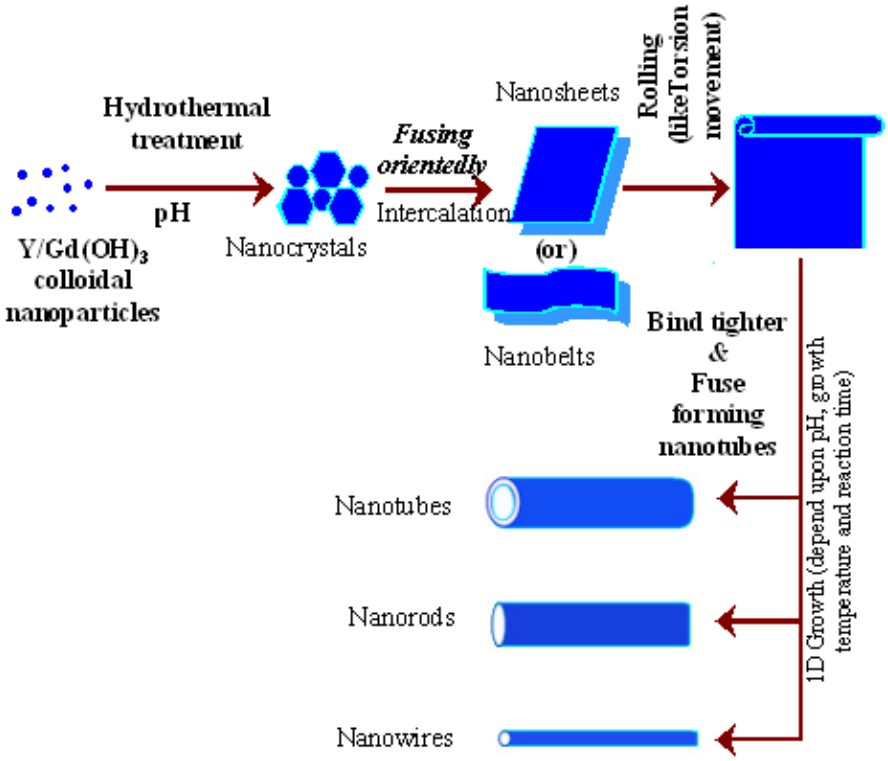

Fig. 5. A schematic diagram of the shape-selective synthesis of doped oxysulfide nanostructures *via* hydrothermal route (template – free method).

2.2 Possible formation mechanism

A schematic diagram of the shape-selective synthesis of doped oxysulfide nanostructures *via* template-free hydrothermal route is shown in Fig. 5. Based on these experimental results and discussions, a possible formation mechanism from nanocrystals to nanowires of hydroxides might be proposed as follows: When the $Y/Gd(NO)_3$ and NaOH solutions are mixed together, the resultant hydroxide nanocrystals can accommodate some Na ions and water molecules between their adjacent surfaces. According to Kerr (Kerr, 1996), these Na ions and water molecules are then exchanged and fused to form nanosheet or nanobelt according to the pH and temperature variation as indicated by the schematic diagram in Fig. 5. As the reaction continues the conformational variation inevitably causes torsional movement within the chains (Colomban, 1999; Mazerolles, 1999), causing the nanosheet / nanobelt to roll up. Because the thin lamellar nanosheet / nanobelt has very good flexibility, they curl and buckle with appropriately 45 degree rotation. As the curling continues, they bind tighter and fuse together at the two edges to form a nanotube with a cylindrical cross section. Furthermore, nanorods and nanowires are obtained according to reaction time, pH and temperature following the same formation kinetics.

3. Template-assisted method

In order to synthesize one-dimensional nanomaterial into a device, a fabrication method that enables well-ordered nanomaterials with uniform diameter and length is important. Template-directed growth is a nanomaterials fabrication method that uses a template, which has arrays of nanopores with uniform diameter and length that is needed for a device. Template-based growth is commonly a solution or colloidal dispersion based process. It is less expensive and readily scalable to mass production. The diameter, density and length of nanotubes, nanorods and nanowires are easily controlled independently. It also offers the advantage of less contamination and is environmentally benign. However, template-based synthesis slightly suffers from the polycrystalline nature of the resultant nanowires and nanorods, in addition to the difficulties to find appropriate templates with pore channels of desired diameter, length and surface chemistry and to remove the template completely without compromising the integrity of grown nanotubes, nanorods and nanowires and is another cumbersome work. In this work the $Y_2O_2S:Eu^{3+}$ and $Gd_2O_2S:Eu^{3+}$ of highly ordered arrays of super-nanostructures like, nanotubes, nanorods and nanoflowers were synthesized by hydrothermal synthesis *via* template assisted synthesis using commercially available AAO templates [Whatman Nuclepore® Inc., (13 mm diameter, 6 μm thickness)]. In comparison with the bulk, this template assisted nanosynthesis route offer several advantages for property study and practical applications. As a whole, to the best of our knowledge, this is the first attempt to prepare such nanostructures from the zero- to three-dimensional scale using both template – free and template – assisted method for these two sytems.

We have extended the method to the synthesis of various nanostructures like nanotubes, nanorods and nanoflowers preparation using template-assisted hydrothermal technique by varying reaction parameters such as solution pH, solvent temperature, time, etc. The porous AAO templates were immersed into a required amount of $[Y/Gd(CH_3COO)_3 \cdot 4H_2O]$ and $[Eu(CH_3COO)_3 \cdot 4H_2O]$ solution, respectively, and evacuated for about 15 min using a vacuum pump to get rid of bubbles within the nanopores. The template was taken out of the solution, rinsed with distilled water and dried in air. This procedure was repeated several times at regular intervals. Subsequently, the template was put into a Teflon-lined stainless steel autoclave, and the solution of $YEu(CH_3COO)_3$ and $GdEu(CH_3COO)_3$, respectively, followed by addition specific amount of Na_2S. The pH of the reaction solution was adjusted in the range from 6 to 9. After that the autoclave was tightly sealed, heated around 150 – 200 °C for 20 hrs and then allowed to cool down to room temperature naturally. For the synthesis of nanoflower-like structures, hexamethylenetetramine (HMT) was used as surfactant. The as-obtained $Y_2O_2S:Eu^{3+}$ and $Gd_2O_2S:Eu^{3+}$ template was subsequently annealed at 300°C for 1 hr under inert Sulphur atmosphere, respectively, to yield the final product.

Structural studies (XRD) reveal that the products $Y_2O_2S:Eu^{3+}$ and $Gd_2O_2S:Eu^{3+}$ are pure hexagonal phase and they are in good agreement with standard JCPDS [($Y_2O_2S:Eu^{3+}$: JCPDS # 24-1424) and ($Gd_2O_2S:Eu^{3+}$: JCPDS # 2 6-1422)] data (Thirumalai et al, 2008; Thirumalai et al, 2009 a,b) and they are highly single crystalline in nature. The patterns show obviously broadened diffraction peaks compared with the bulk $Y_2O_2S:Eu^{3+}$ and $Gd_2O_2S:Eu^{3+}$ systems, signifying the decrease in size of these crystallites. No peaks attributable to other types of oxysulfide(s) are observed in the XRD patterns, indicating the high purity of the phases obtained. The morphology of the resulting samples synthesized by the hydrothermal

method was studied using SEM. Using the commercially available AAO templates the morphologies of highly oriented nanoarrays of structures like nanotubes, nanorods and nanoflowers of $Y_2O_2S:Eu^{3+}$ and $Gd_2O_2S:Eu^{3+}$ were synthesized. The optimal experimental conditions and resulting morphologies of $Y_2O_2S:Eu^{3+}$ and $Gd_2O_2S:Eu^{3+}$ nanostructures are given in Table – I. Fig. 6(a1-c2) & Fig. 7(a1-c2) show the SEM micrographs of the synthesized $Y_2O_2S:Eu^{3+}$ and $Gd_2O_2S:Eu^{3+}$ nanotubes, nanorods and nanoflowers, respectively. They were found to be single-crystalline in nature.

To investigate the optimized growth of the $Y_2O_2S:Eu^{3+}$ and $Gd_2O_2S:Eu^{3+}$ nanostructures, SEM micrographs shows highly oriented nanotubes, nanorods and nanoflowers, respectively, that were obtained by varying the reaction parameters (pH ~ 6 to 9, 150 – 200 °C, 20 hrs) and its resulting morphological features and crystallanity are found to be good. The studies reveal that by altering the reaction conditions (like solution concentration, pH, temperature and time) the morphology, shape and crystallinity are perfectly controlled. Fig 7(a1, a2) and Fig 8(a1, a2) show, the AAO templates top-view and cross-sections of the as-synthesized $Y_2O_2S:Eu^{3+}$ and $Gd_2O_2S:Eu^{3+}$ nanostructures, respectively. A cluster of nanotube-like arrays of the oxysulfide(s) growth were observed [Fig 7(b1, b2) and Fig 8(b1, b2)] at a pH of 6, 150 °C, 15 hrs. In Fig 7b1 and Fig 8b1 the tube and/or rod-like growth is clearly seen. The nanotubes and/or rods were grown at a pH of 6 – 9, 160 –180 °C, 20 hrs and the cross-section view reveals that the nanopores are perfectly filled. The nanorods are straight and have a uniform diameter of about 80 nm, which is basically equal to the pore size of the AAO template employed. To investigate the effect of solvent concentration on $Y_2O_2S:Eu^{3+}$ and $Gd_2O_2S:Eu^{3+}$ nanostructures, SEM micrographs were obtained at different solvent concentration (using hexamethyltetramine (HMT) as solvent along with water). The results are discussed and presented in Fig 7, 8(c1 and c2) and Table – I. The sample is composed of a large number of nearly uniform flower-like nanostructures to the surface of the AAO template. They are arranged uniformly in a large area. The average size of the as-obtained nanostructure is about 4-5 μm. A closer inspection reveals that the flower is made up of many thin petals, the thickness of which is ~ 30 nm. Fig. 6c2 and 8c2 show the cross-sectional view of SEM image of the $Y_2O_2S:Eu^{3+}$ and $Gd_2O_2S:Eu^{3+}$ nanorod arrays of length around hundred nanometers for the flower-like structures. Every petal is curled and thin, with a smooth surface and a large surface area. We can see a layer of flowers on the surface of the template. Because of these nanocrystalline sheets like small petals, the flower-like structure on the alumina template surface formed by these nanocrystalline sheets may be called nanoflowers. The nanoflower growth is clearly seen and the cross-section reveals that the nanopores are perfectly filled for concentration of 2 mM. Fig. 6(a2, b2, c2) and Fig. 7(a2, b2, c2), show a slightly discrete, unattached and dislocation free nanotube/rod structure in the direction vertical to the AAO template, respectively, which was different from the shared tube/rod wall between the tubes/rods of the AAO template. The nanotube/rod wall was also constituted by many deposited particles with an average particle size of 20 nm. It can be seen that the product obtained by the hydrothermal reaction with the AAO template had three structural configurations: (i) many fine nanoparticles packed to form tubes/rods, (ii) many parallel (iii) slightly discrete and completely dislocation free tubes/rods constituted nanorod-like arrays vertical to the AAO template, respectively. The formation of 1D structure depends greatly on the reaction kinetics. Such 3D structures with high surface areas can be used relevantly as catalysts, molecular sieves and biosensors (Zhang, 2007).

	Experimental Conditions*	Resulting morphologies
$Y_2O_2S:Eu^{3+}$	(pH~6, 150°C, 20h)	Nanotubes
	(pH~7–8, 200°C, 20h)	Nanorods
	(pH~8–9, 120°C, 12h)	Nanoflowers
$Gd_2O_2S:Eu^{3+}$	(pH~6, 150°C, 20h)	Nanotubes
	(pH~7–8, 200°C, 20h)	Nanorods
	(pH~8–9, 120°C, 12h)	Nanoflowers

Table 1. Optimized growth conditions of $Y_2O_2S:Eu^{3+}$ and $Gd_2O_2S:Eu^{3+}$ (Template – assisted Method) nanostructures

*The as-obtained $Y_2O_2S:Eu^{3+}$ and $Gd_2O_2S:Eu^{3+}$ grown on AAO template was subsequently annealed at 300 ^oC for 1 hr under inert (A_2 or N_2) / CS_2 / Sulphur atmosphere to yield the final product.

3.1 Possible formation mechanism

Highly oriented single-crystalline $Y_2O_2S:Eu^{3+}$ and $GdO_2S:Eu^{3+}$ nanotubes, nanorods and nanoflowers were synthesized using a template–assisted (AAO and Au coated AAO templates) hydrothermal technique. While Y/Gd $(CH_3COO)_3.4H_2O$: $Eu(CH_3COO)_3.4H_2O$ as precursors act as sources for Y/Gd : Eu ions, during the reaction process, the NaOH not only plays a role as a solvent for lowering the reaction temperature but also acts as a reactant and it is used for achieving basic environment through hydrolysis. Here, Na_2S is acting as a sulfurizing agent. Controlling the pH and reaction time is a key factor in achieving the morphological control. The porous structure of alumina with positive charged walls attracts the ions having negative charge from the solution leading to a preferential deposition at the walls that further grow towards the core. Supersaturation in the growth region is favorable to an anisotropic growth. The shape of a crystal is determined by the relative specific surface energy of each facet of the crystal. Therefore, the initial deposition of nanocrystals is critical for the formation of aligned nanotubes and nanorods. It is inferred that the AAO template may plays an important role in controlling the pH of the reaction mixture and/or local concentration, which leads to an inhomogeneous concentration distribution and may affect the shape development. Immersing the alumina template in the solution containing surfacant (HMT), the solution impregnated through pores to form nanorods immediately. However, the nanorods were not restricted in the pores anymore and extends to the surface of the alumina template, due to forces of adhesion. This in turn may lead to spreading nanorods out of the pore diameter, leading to the possible formation of nanosheets. The nanosheets so formed over the template surfaces comes in intact with the extended nanorods and try to form a stable structure. This situation may lead to the formation of flowery nanostructures. The schematic of the mechanism for nanotube, nanorod and nanoflower generations are shown in Fig. 8.

In summary, this novel template-free and template-based approach has been developed for growing high yield and highly oriented single crystal $Y_2O_2S:Eu^{3+}$ and $Gd_2O_2S:Eu^{3+}$ nanostructures using hydrothermal growth. The pH, growth temperature, reaction time and

surfactant are mainly determining the shape of the nanostructures. The morphological studies were performed through SEM and TEM for the optimized conditions, which reveals excellent features and are reported. The morphological studies (SEM and TEM) revealed that the nanostructures (0D, 1D, 2D and 3D), with various structures like nanocrystals, nanosheets, nanobelts, nanotubes, nanorods, nanowires and highly oriented nanoarrays (tubes, rods, flowers) successfully synthesized. The $Y_2O_2S:Eu^{3+}$ and $Gd_2O_2S:Eu^{3+}$ nanostructures was further examined by HRTEM, electron diffraction and FFT images are seen to be single-crystalline in nature. Also, the SEM studies of the nanorods over AAO tempalte (template – assisted method) reveal that they are uniformly distributed throughout the surface exhibiting the superiority of the structures. The studies agree to a great extent with the structural studies results. This technique is found to be highly reproducible and can be extended to large area and large scale fabrication systems. Large-area, non-collapsed and highly-oriented $Y_2O_2S:Eu^{3+}$ and $Gd_2O_2S:Eu^{3+}$ nanostructures are expected as ideal functional components for opto-electronic and nanoscale devices of the next generation.

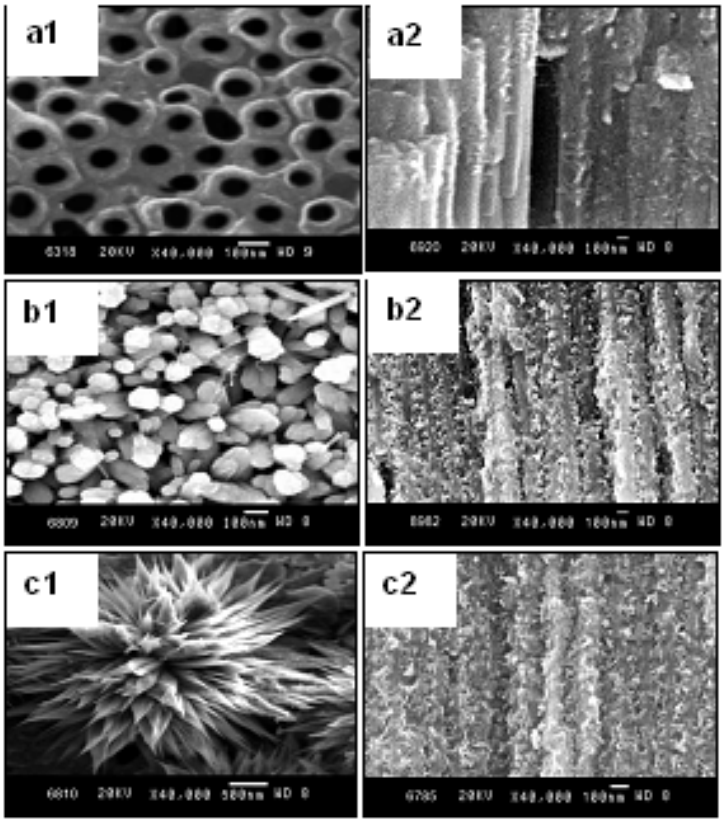

Fig. 6. The SEM images of $Y_2O_2S:Eu^{3+}$ nanostructures (template – assisted method): (a1, a2) Nanotubes, (b1, b2) Nanorods and (c1, c2) Nanoflowers. The SEM micrographs show the cross-sectional views of the samples (a2, b2, c2) corresponding to (a1, b1, c1).

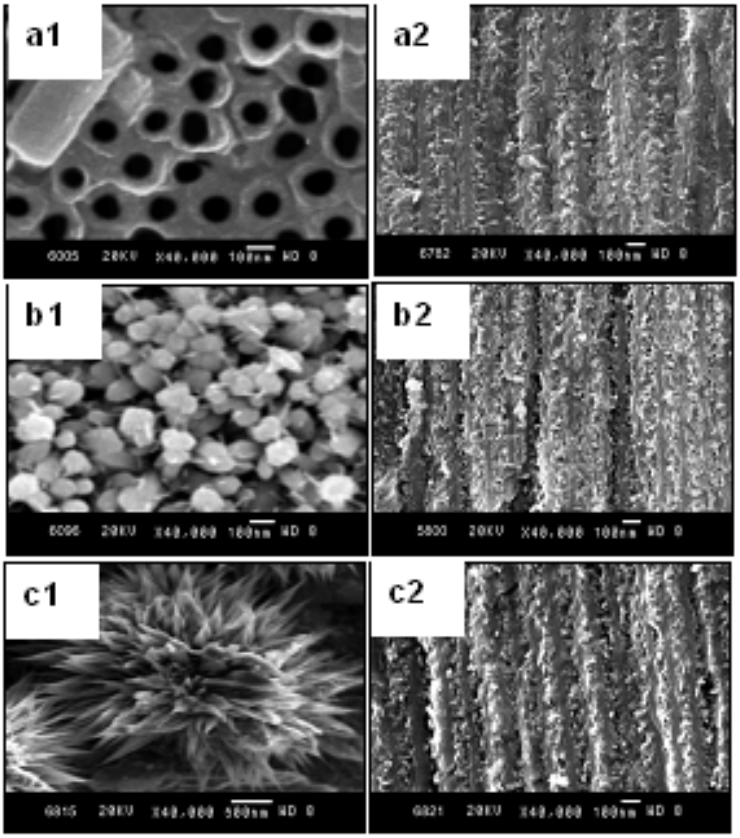

Fig. 7. The SEM images of $Gd_2O_2S:Eu^{3+}$ nanostructures (template – assisted method): (a1, a2) Nanotubes, (b1, b2) Nanorods and (c1, c2) Nanoflowers. The SEM micrographs show the cross-sectional views of the samples (a2, b2, c2) corresponding to (a1, b1, c1).

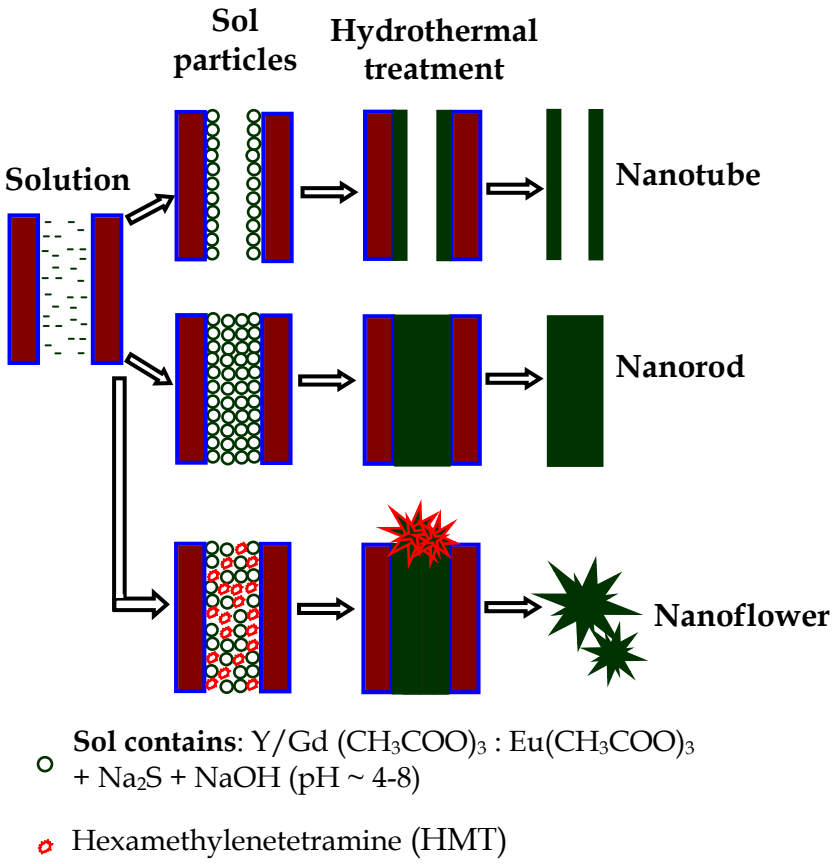

Fig. 8. Schematic illustration of the growth of nanotube, nanorod and nanflower structures by a template-assisted hydrothermal technique.

4. References

Bakovets, V. V.; Levashova, T. M.; Filatova, I. Yu.; Maksimovskii E. A. & Kupcha, A. E. (2008). Vapor phase growth of nanostructured yttrium oxysulfide films. *Inorg. Mater.*, 44., 1., (February & 2008) 67-69, ISSN: 0020-1685.

Bang, J.; Abboudi, M.; Abrams, B. & Holloway, P. H. (2004) Combustion synthesis of Eu-, Tb- and Tm- doped Ln_2O_2S (Ln=Y, La, Gd) phosphors. *J. Lumin.* 106., 3-4., (November & 2003) 177-185, ISSN: 0022-2313.

Chen, X. Y.; Zhuang, H. Z. & Liu G. K.; Li, S. & Niedbala, R. S. (2003). *J. Appl. Phys.*, 94, 1, ISSN 0021-8979.

Chou, T.W. ; Mylswamy, S.; Liu, R.S. & Chuang, S.Z. (2005). Eu substitution and particle size control of Y_2O_2S for the excitation by UV light emitting diodes. *Solid. State.Comm.*, 136., 4., (August 2005) 205-209, ISSN: 0038-1098.

Colomban, P.; Folch, S. & Gruger, A. (1999). Vibrational Study of Short-Range Order and Structure of Polyaniline Bases and Salts. *Macromolecules*. 32., 9., (April & 1999) 3080-3092, ISSN: 0024-9297.

Delgado da Vila, L.; Stucchi, E. B.; Davolos, M. R. (1997). Preparation and characterization of uniform, spherical particles of Y_2O_2S and Y_2O_2S:Eu. *J. Mater. Chem.*, 7., 10., 2113-2116, ISSN: 0959-9428.

Dhanaraj, J.; Jagannathan R. & Trivedi, D. C. (2003). $Y_2O_2S:Eu^{3+}$ nanocrystals—synthesis and luminescent properties. *J. Mater. Chem.,* 13., 7., (May & 2003) 1778-1782, ISSN 0959-9428.

Dhanaraj, J.; Geethalakshmi, M.; Jagannathan, R. and Kutty, T.R.N. (2004). Eu3þ doped yttrium oxysulfide nanocrystals – crystallite size and luminescence transition(s). *Chem. Phys. Lett.,* 387., 1-3., (March & 2004) 23-28, ISSN: 0009-2614.

Fu, Z.; Geng, Y.; Chen, H.; Zhou, S.; Yang, H. K. & J. H. Jeong, (2008). Combustion synthesis and luminescent properties of the Eu^{3+}-doped yttrium oxysulfide nanocrystalline. *Opt.Mater.* 31., 1., (September & 2008) 58-62., ISSN: 0925-3467.

Guo, C.; Luan, L.; Chen, C.; Huang D. & Su, Q. (2008). Preparation of $Y_2O_2S:Eu^{3+}$ *phosphors* by a novel *decomposition* method. *Mater. Lett.* 62., 4-5., (February & 2008) 600-602, ISSN: 0167-577X.

Hang, T.; Liu, Q.; Mao, D. & Chang, C. (2008). Long lasting behavior of $Gd_2O_2S:Eu^{3+}$ phosphor synthesized by hydrothermal routine. *Mater. Chem. Phys.*, 107., 1., (January & 2008) 142-147, ISSN: 0254-0584.

Hirai, T.; Hirano, T. & Komasawa, I. (2002). Preparation of $Gd_2O_3 : Eu^{3+}$ and $Gd_2O_2S : Eu^{3+}$ Phosphor Fine Particles Using an Emulsion Liquid Membrane System. *J. Colloid. Inter. Sci.* 253., 1., (September & 2002) 62-69, ISSN: 0021-9797.

Kerr, T. A.; Wu, H. & Nazar, L. F. Concurrent Polymerization and Insertion of Aniline in Molybdenum Trioxide: Formation and Properties of a $[Poly(aniline)]_{0.24}MoO_3$ Nanocomposite. (1996). *Chem. Mater.* 8., 8., (August 1996) 2005-2015, ISSN: 0897-4756.

Kong, Y. C.; Yu, D. P.; Zhang, B.; Fang, W. & Feng, S. Q. (2001). *Appl. Phys.Lett.*, 78., 407., ISSN 0003-6951.

Koskenlinn, M.; Leskela M. & Niinisto, L. (1976). Synthesis and Luminescence Properties of Europium-Activated Yttrium Oxysulfide Phosphors. *J. Electrochem. Soc.* 123., 1., (January & 1976) 75-78., ISSN: 0013-4651.

Kuang, J.; Liu, Y. & Yuan, D. *Electrochem.* (2005). Preparation and Characterization of $Y_2O_2S:Eu^{3+}$ Phosphor via One-Step Solvothermal Process. *Solid. State. Lett.*, 8., 9., (July & 2005),H72-H74, ISSN: 1099-0062.

Lei, B.; Liu, Y.; Zhang, J.; Meng, J.; Man, S. & Tan, S. (2010). Persistent luminescence in rare earth ion-doped gadolinium oxysulfide phosphors. *J. Alloys. Comp,* 495., 1., (February and 2010) 247-253, ISSN: 0925-8388.

Leskelä M. & Niinistö, L. (1976). Solid solutions in the rare-earth oxysulfide series. *J. Solid. State. Chem.* 19., 3., (November 1976) 245-250, ISSN: 0022-4596.

Li, W; Liu, Y; & Ai, P. (2010). Synthesis and luminescence properties of red long-lasting phosphor $Y_2O_2S:Eu^{3+}$, Mg^{2+}, Ti^{4+} nanoparticles. *Mater. Chem. Phys.,* 119, 1-2., (January & 2010) 52-56, ISSN: 0254-0584.

Liu, Y. & Kuang, J. (2010). Intense visible luminescence from Nd^{3+}-doped yttrium oxysulfide. *J. Lumin.* 130., 3., (March and 2010) 351-354, ISSN: 0022-2313.

Mazerolles, L.; Floch, S. & Colomban, P. (1999). Study of Polyanilines by High-Resolution Electron Microscopy. *Macromolecules*. 32., 25., (November & 1999) 8504-8508, ISSN: 0024-9297.

Mao, S.; Liu, Q.; Gu, M.; Mao D. & Chang, C. (2008). Long lasting phosphorescence of Gd_2O_2S:Eu,Ti,Mg nanorods via a hydrothermal routine. *J. Alloys and Comp.,* 465., 1-2., (October & 2008) 367-374, ISSN: 0925-838.

Mikami, M. & Oshiyama, A. (1998). First-principles band-structure calculation of yttrium oxysulfide.*Phys. Rev. B,* 57., 15., (April &1998) 8939-8944, ISSN: 1098-0121.

Nakkiran, A.; Thirumalai, J.; & Jagannathan, R. (2007). Luminescence blinking in Eu^{3+} doped yttrium oxysulfide ($Y_2O_2S:Eu^{3+}$) quantum-dot ensembles: Photo-assisted relaxation of surface state(s). *Chem. Phys. Lett.*, 436., 1-3., (February and 2007)155-161, ISSN: 0009-2614.

Pan, Z. W.; Dai, Z. R. & Wang, Z. L. (2001). Nanobelts of Semiconducting Oxides. *Science.* 291., 5510., (March & 2001) 1947-1949, ISSN: 0036-8075.

Sabot, J. L. & Maestro, P. (1995). *Kirk-Othmer Encyclopedia of Chemical Technology, Concise, 4th Edition,* John Wiley & Sons, IV-edn, ISBN: 0-471-41961-3.

Tseng, Y.H.; Chiou, B.S.; Peng, C.C. & Ozawa, L. (1998). Spectral properties of Eu^{3+}-activated yttrium oxysulfide red phosphor. *Thin Solid Films.,* 330., 2., (September & 1998) 173-177, ISSN: 0040-6090.

Thirumalai, J.; Jagannathan, R. & Trivedi, D.C. (2007). $Y_2O_2S:Eu^{3+}$ nanocrystals, a strong quantum-confined luminescent system. *J. Lumin.* 126., 2., (October and 2007) 353-358, ISSN: 0022-2313.

Thirumalai, J.; Chandramohan, R.; Sekar M.& Rajachandrasekar, R. (2008). Eu^{3+} doped yttrium oxysulfide quantum structures — structural, optical and electronic properties. *J. Nanopart. Res.* 10., 3., (August & 2007) 455-463, ISSN: 1388-0764.

Thirumalai, J.; Chandramohan, R.; Divakar, R.; Mohandas, E.; Sekar, M. & Parameswaran, P. (2008). Eu^{3+} doped gadolinium oxysulfide (Gd_2O_2S) nanostructures —synthesis and optical and electronic properties. *Nanotechnology.* 19., 39., (October & 2008) 395703-5, ISSN: 0957-4484.

Thirumalai, J.; Chandramohan, R.; Auluck, S.; Mahalingam, T. & Srikumar, S. R. Controlled synthesis, optical and electronic properties of Eu^{3+} doped yttrium oxysulfide (Y_2O_2S) nanostructures. (2009a). *J. Colloid. Interface. Sci.* 336., 2., (August & 2009) 889-897, ISSN: 0021-9797.

Thirumalai, J.; Chandramohan, R.; Valanarasu, S.; Vijayan T. A.; Somasundaram, R. M.; Mahalingam, T. & Srikumar, S. R. (2009b). Shape-selective synthesis and opto-electronic properties of Eu^{3+}-doped gadolinium oxysulfide nanostructures. *J. Mater. Sci.* 44., 14., (July & 2009) 3889-3899, ISSN: 0022-2461.

Wang, X. & Li, Y. (2003). Rare-Earth-Compound Nanowires, Nanotubes, and Fullerene-Like Nanoparticles: Synthesis, Characterization, and Properties.*Chem. Eur. J.* 9., 22., (November & 2003), 5627-5635, ISSN: 0947-6539.

Wang, X.; Sun, X.; Yu, D.; Zou, B. & Li, Y. D. (2003). Rare earth compound Nanotubes. *Adv. Mater.* 15., 17., (September & 2003) 1442-1445, ISSN: 0935-9648.

Xixian, L.; Wanghe, C. & Mingming, X. (2006). Preparation of nano Y_2O_2S:Eu phosphor by ethanol assisted combustion synthesis method. *J. Rare. Earths.*, 24., 1., (February & 2006) 20-24, ISSN: 1002-0721.

Yeboah, C. & Pistorius, S. (2000). Monte Carlo studies of the exit photon spectra and dose to a metal/phosphor portal imaging screen.*Med. Phys.* 27., 2., (February & 2000) 330-339, ISSN: 0094-2405.

Yu, T.; Zhu, Y.; Xu, X.; Shen, Z.; Chen, P.; Lim, C-T.; Thong, J.T-L.& Sow, C-H. (2005). Controlled Growth and Field-Emission Properties of Cobalt Oxide Nanowalls. *Adv. Mater.* 17., 13., (July & 2005) 1595-1599, ISSN: 0935-9648.

Zhang, B. P.; Binh, N. T.; Wakatsuki, K.; Segawa, Y.; Yamada, Y.; Usami, N.; Kawasaki, M. & Koinuma, H. (2004). *Appl. Phys. Lett.*, 84., 4098, ISSN 0003-6951.

Zhang, C.; Tao, F.; Liu, G-Q.; Yao, L- Z. & Cai, W-L. (2008). Hydrothermal synthesis of oriented MnS nanorods on anodized aluminum oxide template. *Mater. Lett.* 62., 2., (January & 2008) 246-248, ISSN: 0167-577X.

Zhang, D.; Fu, H.; Shi, L.; Fang, J. & Li, Q. (2007). Carbon nanotube assisted synthesis of CeO_2 nanotubes. *J. Solid. State. Chem.*, 180., 2., (February 2007) 654-660, ISSN: 0022-4596.

Zhang, J.; Sun, L.; Yin, J.; Su, H.; Liao, C. & Yan, C. (2002). Control of ZnO Morphology via a Simple Solution Route. *Chem. Mater.* 14., 10., (September & 2002) 4172-4177, ISSN: 0897-4756.

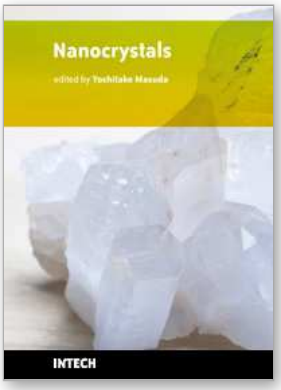

Nanocrystals

Edited by Yoshitake Masuda

ISBN 978-953-307-126-8
Hard cover, 326 pages
Publisher Sciyo
Published online 06, October, 2010
Published in print edition October, 2010

This book contains a number of latest research developments on nanocrystals. It is a promising new research area that has received a lot of attention in recent years. Here you will find interesting reports on cutting-edge science and technology related to synthesis, morphology control, self-assembly and application of nanocrystals. I hope that the book will lead to systematization of nanocrystal science, creation of new nanocrystal research field and further promotion of nanocrystal technology for the bright future of our children.

How to reference

In order to correctly reference this scholarly work, feel free to copy and paste the following:

Rathinam Chandramohan Pillai, Jagannathan Thirumalai and Thirukonda Anandha Vijayan (2010). Synthesis and Morphology Control of Eu3+ Doped M2O2S [M=Y, Gd] Nanostructures, Nanocrystals, Yoshitake Masuda (Ed.), ISBN: 978-953-307-126-8, InTech, Available from: http://www.intechopen.com/books/nanocrystals/synthesis-and-morphology-control-of-eu3-doped-m2o2s-m-y-gd-nanostructures

INTECH
open science | open minds

InTech Europe
University Campus STeP Ri
Slavka Krautzeka 83/A
51000 Rijeka, Croatia
Phone: +385 (51) 770 447
Fax: +385 (51) 686 166
www.intechopen.com

InTech China
Unit 405, Office Block, Hotel Equatorial Shanghai
No.65, Yan An Road (West), Shanghai, 200040, China
中国上海市延安西路65号上海国际贵都大饭店办公楼405单元
Phone: +86-21-62489820
Fax: +86-21-62489821